HHS Public Access

Author manuscript

J Mol Cell Cardiol. Author manuscript; available in PMC 2020 March 01.

Published in final edited form as:

J Mol Cell Cardiol. 2019 May ; 130: 49–58. doi:10.1016/j.yjmcc.2019.03.015.

Adenosine Kinase attenuates cardiomyocyte microtubule stabilization and protects against pressure overload-induced hypertrophy and LV dysfunction

John Fassett[1,&,*], **Xin Xu**[3,&], **Dongmin Kwak**[2], **Guangshuo Zhu**[2], **Erin K Fassett**[1], **Ping Zhang**[2], **Huan Wang**[2], **Bernd Mayer**[1], **Robert J. Bache**[2], and **Yingjie Chen**[2,*]

[1]Department of Pharmacology and Toxicology, University of Graz, Graz, 8010 Austria

[2]Cardiovascular Division and Lillehei Heart Institute; University of Minnesota, Minneapolis, MN 55455, USA

[3]Department of Exercise Rehabilitation, Shanghai University of Sport, Shanghai 200438, China

Abstract

Adenosine exerts numerous protective actions in the heart, including attenuation of cardiac hypertrophy. Adenosine kinase (ADK) converts adenosine to adenosine monophosphate (AMP) and is the major route of myocardial adenosine metabolism, however, the impact of ADK activity on cardiac structure and function is unknown. To examine the role of ADK in cardiac homeostasis and adaptation to stress, conditional cardiomyocyte specific ADK knockout mice (cADK$^{-/-}$) were produced using the MerCreMer-lox-P system. Within 4 weeks of ADK disruption, cADK$^{-/-}$ mice developed spontaneous hypertrophy and increased β-Myosin Heavy Chain expression without observable LV dysfunction. In response to 6 weeks moderate left ventricular pressure overload (transverse aortic constriction;TAC), wild type mice (WT) exhibited ~60% increase in ventricular ADK expression and developed LV hypertrophy with preserved LV function. In contrast, cADK$^{-/-}$ mice exhibited significantly greater LV hypertrophy and cardiac stress marker expression (atrial natruretic peptide and β-Myosin Heavy Chain), LV dilation, reduced LV ejection fraction and increased pulmonary congestion. ADK disruption did not decrease protein methylation, inhibit AMPK, or worsen fibrosis, but was associated with persistently elevated mTORC1 and p44/42 ERK MAP kinase signaling and a striking increase in microtubule (MT) stabilization/ detyrosination. In neonatal cardiomyocytes exposed to hypertrophic stress, 2-chloroadenosine (CADO) or adenosine treatment suppressed MT detyrosination, which was reversed by ADK inhibition with iodotubercidin or ABT-702. Conversely, adenoviral over-expression of ADK augmented CADO destabilization of MTs and potentiated CADO attenuation of cardiomyocyte hypertrophy. Together, these findings indicate a novel adenosine receptor-independent role for ADK-mediated adenosine metabolism in cardiomyocyte microtubule dynamics and protection against maladaptive hypertrophy.

[*]Corresponding author Address for correspondence: Yingjie Chen, MD, PhD, University of Minnesota, Mayo Mail Cod 508, 420 Delaware St. SE, Minneapolis, MN55455, Tel: (612) 624-8970, Fax: (612) 626-4411, chenx106@tc.umn.edu; John Fassett, PhD, University of Graz, Dept of Pharmacology and Toxicology, Humboldtstrasse 46, Graz, Austria, 8010, Tel: +43 316 3805560, john.fassett@uni-graz.at.

[&]Equal contribution to this work

Disclosures: The authors have no conflicts of interests to disclose

Keywords

adenosine kinase; microtubules; detyrosinated tubulin; heart failure

Introduction

Adenosine exerts acute cardio-protective actions such as preconditioning[1, 2] and coronary vasodilation[3], and counteracts several chronic, maladaptive processes, including inflammation[4, 5], fibrosis[6], and cardiac hypertrophy[7–10]. In addition, adenosine suppresses cardiomyocyte microtubule stabilization and detyrosination [11], a cytoskeletal response to hypertrophic stress that has been shown to increase viscous load on the myofilament[12–15] and alter mechanotransduction-dependent ROS and calcium signaling[16–18]. While activation of cell surface adenosine receptors (A1, A2A, A2B, and A3) are responsible for the vast majority of adenosine's cardioprotective effects, adenosine also exerts non-receptor-dependent actions that can protect against ischemia reperfusion injury[19] and attenuate cardiomyocyte hypertrophy[20].

Besides activating adenosine receptors, adenosine is taken up by cardiomyocytes and phosphorylated by adenosine kinase (ADK) or degraded by adenosine deaminase[21]. In support of a non-receptor-dependent mechanism of attenuating hypertrophy, adenosine (10μM) or 2-chloroadenosine (CADO; 5 μM) mediated reduction of phenylephrine-induced protein synthesis and cell enlargement in neonatal rat cardiomyocytes was completely reversed by pharmacological inhibition of adenosine kinase (ADK)[20]. The ADK-dependent, adenosine receptor-independent attenuation of hypertrophy by exogenous adenosine in neonatal cardiomyocytes raises the intriguing possibility that ADK may exert similar growth inhibitory effects in the adult heart through metabolism of endogenous, intracellular adenosine.

Due to well-established protective effects of adenosine, ADK inhibitors are being considered as an approach to elevate interstitial adenosine levels to treat inflammatory or neurological disorders[22–24]. In the heart, ADK activity accounts for ~90% of myocardial adenosine metabolism[21] and plays a major role in regulating intracellular and extracellular adenosine concentration[25]. However, despite the important roles of adenosine in the heart, the in vivo impact of cardiomyocyte ADK activity and endogenous adenosine metabolism on cardiac homeostasis and hypertrophy is unknown. In this study, conditional cardiomyocyte-specific ADK knockout mice were produced to investigate the in vivo role of ADK in cardiac homeostasis, cytoskeletal dynamics and adaptation to left ventricular pressure overload. Additionally, pharmacological ADK inhibitors and ADK over-expression were used in neonatal rat cardiomyocytes to further examine the role of ADK and adenosine in cardiomyocyte microtubule dynamics.

Methods

Animals and transverse aortic constriction (TAC).

This study was approved by the Institutional Animal Care and Use Committee of University of Minnesota. Animals were housed in an air-conditioned room with a 12-h:12-h light-dark cycle, received standard rodent chow, and drank tap water. Floxed ADK mice ($ADK^{f/f}$) in a c57Bl6/129 background were crossed to Myh6-mer-cre-mer mice ($Myh6\text{-}cre^{+/+}$) [26] (Kindly provided by Jeffrey Robbins; Cincinnati Childrens Hospital), also in the c57Bl/6 background. Offspring were backcrossed to create $ADK^{f/f}$ /$Myh6\text{-}cre^{-+/}$ and $ADK^{f/f}$ /$Myh6\text{-}cre^{-/-}$ mice, which were used as breeders to produce litters of 50% $ADK^{f/f}$ /$Myh6\text{-}cre^{-/-}$ and 50% $ADK^{f/f}$ /$Myh6\text{-}cre^{+/-}$. Male littermates were treated with tamoxifen to induce cardiomyocyte specific excision of ADK exon 7 of the ADK gene (designated $cADK^{-/-}$). $ADK^{f/f}$ /$Myh6\text{-}cre^{-/-}$littermates treated with tamoxifen were used as controls (designated as WT). 4 weeks after the last tamoxifen injections, cADK KO and WT mice were used for sham surgery or transverse aortic constriction (TAC) as previously described [27].

Echocardiography and LV hemodynamics.

Echocardiographic images were obtained using a Visual Sonics high resolution Vevo 770 system as previously described [28]. A 1.2 Fr. pressure catheter (Scisense Inc. Ontario Canada) was used to measure LV pressures. Further details are provided in the online supplement.

Western blot.

Triton x-100 soluble and insoluble protein lysates of mouse ventricles were prepared as previously described[11]. The following antibodies were used: phospho-$mTOR^{ser2448}$, total mTOR, phospho-$p70S6\ kinase^{Thr389}$, total p70S6 kinase, phospho-$4E\text{-}BP^{Thr37/46}$, total 4E-BP1, phospho-$AMPK^{Thr172}$, total AMPK, methyl-arginine, (Cell Signaling; Beverly, MA), ADK, (Santa Cruz Biotechnology; Santa Cruz, CA), atrial natruretic peptide (Peninsula biolabs; San Carlos, CA), Desmin (Abcam; Cambridge, MA), and detyrosinated tubulin (Abcam; Cambridge, MA and Upstate Biotechnology; Lake Placid, NY), β-MHC, α-sarcomeric actin, β-actin (Sigma; St Louis, MO).

Neonatal Cardiomyocyte culture.

NRVMs were isolated from 2–4 day-old Sprague-Dawley rats by enzymatic digestion and separated from non-muscle cells on a discontinuous Percoll gradient as previously described[11].

MT isolation.

Microtubule isolation and subcellular fractionation: Microtubule fractions were isolated from mouse ventricles in glycerol based microtubule stabilization buffer as previously described [11, 14]. Further details are provided in the online supplement.

Immunostaining.

NRVMs were fixed in −20°C methanol and microtubules were detected using anti-alpha tubulin (Sigma Aldrich. St Louis, MO) and rabbit anti-detyrosinated tubulin (Abcam;

cambridge, UK), as previously described. **Materials.** 2-chloroadenosine, Iodotubercidin and ABT-702 were from Tocris (Bristol;UK). Adenosine was from Sigma Aldrich.

Data and Statistical Analyses.

All values were expressed as mean ± standard error of the mean (SEM). Statistical significance was defined as $P < 0.05$. One-way analysis of variance (ANOVA) was used to test each variable for differences among the treatment groups with StatView (SAS Institute Inc). If ANOVA demonstrated a significant effect, post hoc pairwise comparisons were made with two tailed Students T-test. Data that was not normally distributed were analyzed using the Mann-Whitney test.

Results

ADK disruption causes spontaneous cardiac hypertrophy.

$ADK^{f/f}$ /Myh6-$cre^{-+/}$ and $ADK^{f/f}$ /Myh6-$cre^{-/-}$ mice were treated with tamoxifen to excise exon 7 and create a frameshift mutation in the ADK gene to produce cardiomyocyte specific ADK knockout mice ($cADK^{-/-}$) (figure 1A). 4 weeks after the last tamoxifen injection, ADK expression was reduced by 95% in the hearts of $cADK^{-/-}$ mice, but unaffected in other organs (figure 1B). $cADK^{-/-}$ mice developed significantly increased heart to body weight ratio (figure 1C), left ventricular (LV) weight, right ventricular (RV) weight, and left (LA) and right atrial (RA) weight to body weight ratios without observable effects on other organs (online supplement figure S1A, S1B). In addition, $cADK^{-/-}$ hearts exhibited strong expression of the cardiac hypertrophic stress marker, β-MyHC, as compared to WT mice (figure 1D, E). Despite the significant increase in hypertrophy in $cADK^{-/-}$ hearts, echocardiography measurements demonstrated no difference between WT and $cADK^{-/-}$ mice in LV chamber dimensions or function (online supplement figure S1C).

Cardiomyocyte ADK expression attenuates pressure overload induced hypertrophy.

To examine the impact of cardiomyocyte ADK expression on adaptation to hypertrophic stress, moderate pressure overload was applied to WT and $cADK^{-/-}$ mice via transverse aortic constriction (TAC; 26 gauge needle, ~110 mmHg systolic aortic pressure) for 6 weeks. In comparison to WT mice, $cADK^{-/-}$ mice developed greater TAC induced increases in left ventricular weight/BW ratio (94% in $cADK^{-/-}$; 70% in WT) (figure 2A), left atrial weight/BW (238% in $cADK^{-/-}$; 151% in WT) (figure 2B), and right ventricular weight/BW (57% in $cADK^{-/-}$; 35% in WT) (figure 2C), and (Box plots for non-normally distributed data in Supplemental figure S2A), indicating that in addition to increased basal hypertrophy, TAC-induced cardiac hypertrophy is also exaggerated in $cADK^{-/-}$ mice. At the same time, sirus red staining demonstrated no significant difference between WT and $cADK^{-/-}$ mice in myocardial fibrosis (figure 2D). WGA staining of heart sections revealed that $cADK^{-/-}$ cross-sectional area of $cADK^{-/-}$ cardiomyocytes was approximately 40% greater than WT cardiomyocytes under basal conditions and approximately 30% greater than WT after TAC (figure 2E, F), indicating that increased heart weight in $cADK^{-/-}$ mice is largely due to increased cardiomyocyte enlargement.

Interestingly, moderate TAC caused an approximate 60% increase in ADK expression in WT mice (figure 2G, H) and these mice exhibited only modest induction of pathological hypertrophy markers ANP and β-MHC (figure 2G, I, J). In contrast, cADK$^{-/-}$ hearts exhibited a striking increase in ANP and greatly exaggerated β-MHC expression in response to TAC (figure 2G,I, J). These data indicate that cardiomyocyte ADK expression attenuates pressure overload induced cardiomyocyte hypertrophy and activation of the fetal gene program.

cADK$^{-/-}$ mice develop LV dysfunction in response to moderate TAC.

In WT mice exposed to moderate TAC, cardiac hypertrophy developed without pathologic changes in LV chamber dimensions and preserved LV ejection fraction (figure 3A–C). In contrast, cADK$^{-/-}$ mice developed LV dilation (figure 3A, B and S2B) and exhibited lower ejection fraction (figure 3C) in response to the same stress. cADK$^{-/-}$ mice also exhibited significantly increased lung weight in comparison to WT mice, a sign of congestive heart failure (figure 3D). Invasive hemodynamic measurements showed that LV end-systolic pressure increased equally in WT and cADK$^{-/-}$ mice, but LV end-diastolic pressure was significantly greater in cADK$^{-/-}$ mice, indicative of impaired LV relaxation (figure 3E, F). In addition, while LV relaxation rate (-dP/dT min) of WT mice increased in response to moderate TAC, this was not observed in cADK$^{-/-}$ mice (figure 3G–H). Thus, cardiomyocyte ADK activity appears important for structural and functional adaptation to systolic overload.

ADK regulates Cardiac mTORC1 and p44/42 ERK MAP kinase signaling.

Based on our previous observation that adenosine attenuates sustained mTORC1 and p44/42 ERK signaling in neonatal rat cardiomyocytes through an ADK dependent mechanism[20], we examined the potential involvement of these pathways in cADK$^{-/-}$ cardiac hypertrophy. Phosphorylation of mTORC1 substrates p70S6k^{Thr389} and 4E-BP$^{Ser36/47}$ appeared higher in cADK$^{-/-}$ hearts than WT hearts under basal conditions (figure 4A–D). After TAC, phosphorylation of these mTOR targets increased significantly in both WT and cADK$^{-/-}$ hearts (figure 4A–D) and less difference in p70S6k^{Thr389} phosphorylation was observed between WT and cADK$^{-/-}$ hearts, due to greater relative increase in p70S6k phosphorylation in WT hearts. Phosphorylation of 4E-BP$^{Ser37/46}$ however, remained significantly greater in cADK$^{-/-}$ hearts than WT hearts after TAC. Interestingly, protein levels of p70S6k and 4E-BP were also elevated in cADK$^{-/-}$ hearts as compared to WT hearts, which accounted for much of the increased phosphorylated levels of these proteins (figure 4A, G–4I) Another pro-hypertrophic signaling pathway, p44/42 ERK1/2, was also increased in cADK$^{-/-}$ hearts under both basal and TAC conditions, due to stronger p44/42 ERK1/2 expression and subsequently higher levels of phospho-p44/42 ERK$^{Thr202/204}$ (figure 4A, E, J). Phosphorylation of a different MAP kinase however, p38 $^{Thr182/Tyr184}$, appeared slightly reduced by ADK disruption under basal conditions, and no difference was observed between cADK$^{-/-}$ and WT mice after TAC (figure 4A, F, K). Because cardiac mTORC1 and ERK activity promote hypertrophy[29, 30], the chronic up-regulation of these signaling pathways likely contributes to the greater hypertrophy in cADK$^{-/-}$ mice. On the other hand, both of these pathways are important for physiological adaptation to pressure overload[31, 32], so additional factors likely contribute to the exacerbated LV dysfunction observed in cADK $^{-/-}$ mice.

AMPK activation and protein methylation in cADK$^{-/-}$ hearts.

ADK produces AMP, an activator of AMP-activated protein kinase (AMPK). AMPK inhibits mTORC1 signaling and is important for cardiac adaptation to pressure overload [33]. Phosphorylation of AMPK^{Thr172} (an indicator of AMPK activation), appeared higher in cADK$^{-/-}$ hearts under basal conditions, but this was due to increased AMPK expression in cADK$^{-/-}$ hearts, so that the fraction of AMPK phosphorylated was slightly lower relative to WT hearts. No differences in AMPK phosphorylation were observed between WT and cADK$^{-/-}$ hearts after TAC (online supplement; figure S3). High intracellular adenosine levels can inhibit S-adenosylhomocysteine hydrolase, leading to accumulation of S-adenosylhomocysteine, an inhibitor of methyltransferase reactions. ADK dependent removal of intracellular adenosine is believed to be important for maintaining methylation reactions [34]. To examine protein methylation, we measured methylated arginine levels in WT and cADK$^{-/-}$ hearts. Unexpectedly, methylated protein content was higher in cADK$^{-/-}$ hearts **(**online supplement; figure S3**)**, indicating that insufficient methylation does not underlie the maladaptive cardiac phenotype of cADK$^{-/-}$ mice.

ADK regulation of cardiomyocyte microtubules.

Previously, we demonstrated that extracellular adenosine attenuates cardiomyocyte microtubule stabilization and can decrease detyrosinated tubulin content[11]. Microtubule stabilization/accumulation has been shown to contribute to cardiomyocyte contractile dysfunction in the setting of pressure overload [11, 13, 14, 35, 36] and recently, microtubule detyrosination was implicated in cardiomyocyte contractile impairment in human heart failure of multiple etiologies[15]. Levels of non-polymerized (Free) tubulin and cold labile, dynamic microtubules (MTs) represent approximately 50% and 30–40% of total tubulin, respectively, in mouse heart microtubule preparations. Cold stable, triton soluble MTs associated with the cell membrane fraction (memb), and triton insoluble cytoskeletal fractions (CSK), represent approximately 10–15% and 2–5% respectively, of the remaining pools of tubulin. Tubulin levels in the membrane and cytoskeletal fractions increase significantly in pressure overload induced heart failure and correlate strongly with LV dysfunction[37]. Under basal conditions, cADK$^{-/-}$ and WT hearts exhibited no significant differences in Free and cold-labile MTs (figure 5B–D), but did exhibit significantly greater levels of membrane-associated tubulin (Figure 5B,E) and CSK tubulin (figure 5B, F) than WT hearts. In response to moderate TAC, WT hearts did not exhibit a significant increase in tubulin in any subcellular MT fraction (figure 5B–F). In cADK$^{-/-}$ hearts, cold-labile microtubules (MTs) increased to a significantly higher level than WT hearts (figure 5B, D) and the difference between WT and cADK$^{-/-}$ hearts in membrane associated tubulin levels also became slightly greater after TAC.

Detyrosination of alpha tubulin is a post-translational modification of long-lived microtubules[38] that has been shown to alter subcellular trafficking [39, 40], disturb calcium dynamics[17], and increase mechanical load on the myofilament [13, 15]. Western blot analysis revealed significantly greater levels of detyrosinated tubulin in cADK$^{-/-}$ hearts than WT hearts (figure 5G–K), particularly in the MT, Memb, and CSK fractions after TAC. These findings indicate that ADK activity attenuates cardiac microtubule stabilization and detyrosination and prevents aberrant subcellular MT distribution.

The extent to which MTs are depolymerized is generally believed to be a function of their longeivity. However, changes in expression of tubulin carboxypeptidases and tubulin tyrosine ligases[41], the enzymes which directly modify tubulin tyrosination, might also contribute to altered levels of detyrosinated tubulin. Therefore, we examined the expression of Vasohibin1(VASH1), a recently identified tubulin carboxypeptidase[42, 43], and tubulin tyrosine ligase in WT and cADK$^{-/-}$ hearts. Western blot analysis revealed no significant changes in expression of VASH1, while TTL levels were increased in cADK$^{-/-}$ hearts under basal conditions and trended higher after TAC (online supplementfigure S4). These results indicate that ADK-mediated changes in microtubule detyrosination are not likely due to changes in expression levels of the known tubulin tyrosine regulating proteins.

In addition to increasing cardiac microtubule stability, ADK disruption also increased levels of cytoskeletal proteins, β-actin and desmin under basal conditions (figure 5L–N). While β-actin content became equivalent in cADK$^{-/-}$ and WT hearts after TAC, due to a significant increase only in WT hearts (figure 5L, M), desmin levels increased significantly above basal levels in cADK$^{-/-}$ hearts (figure 5L, N).

Adenosine metabolism by ADK diminishes detyrosinated microtubules.

To further define the role(s) of ADK and adenosine in cardiomyocyte microtubule dynamics, we used a neonatal cardiomyocyte hypertrophy model, in which phenylephrine promotes hypertrophy and microtubule stabilization/detyrosination[11]. As previously demonstrated[11], co-treatment with 2-chloroadenosine (CADO; an adenosine deaminase resistant adenosine analogue) has little effect on free tubulin(figure 6A, B**)** attenuates the phenylephrine-induced increase triton insoluble cytoskeletal (CSK) tubulin as well as detyrosinated tubulin (glu-tubulin), as indicated by western blot analysis (figure 6A, C, D, E**).** Inhibition of ADK activity using iodotubercidin (ITU; 0.3μM) significantly reversed the effects of CADO on microtubules, particularly in the cytoskeletal fraction (**6D** and **E**). Interestingly, while adenosine receptor antagonism using 8-phenyltheophylline (8-PT) appeared to block CADO reduction of CSK tubulin, it did not block CADO reduction of detyrosinated tubulin (figure 6A–E**)** and (Supplementary data Figure S6A). Immunofluorescent analysis (figure 6F) also showed that CADO suppression of microtubule detyrosination was reversed by ITU, but not by adenosine receptor antagonism with 8-PT. In addition, selective A1, A2A, and A2B adenosine receptor antagonists were ineffective at blocking CADO effects on MTs, and A3 receptor antagonism actually appeared to potentiate CADO inhibition of MT stability. (Supplementary data S5A-H). These results indicate that ADK activity mediates CADO destabilization of MTs. Similar to CADO, 10μM adenosine reduced levels of detyrosinated MTs, and this was reversed by ABT-702 (Supplementary data S6B) an ADK inhibitor mechanistically distinct from ITU. To examine the potential of CADO to diminish detyrosinated MTs, independent of its anti-hypertrophic actions, we allowed cardiomyocytes to hypertrophy for 48 hours, and then added CADO for an additional 24 hours. Importantly, CADO treatment depleted detyrosinated MTs without significantly affecting cell area, and this was blocked by ADK inhibition with ABT-702 (figure 6C, D). These results suggest adenosine metabolism by ADK can re-establish dynamic MTs in hypertrophied cardiomyocytes and these effects occur independently from adenosine attenuation of hypertrophy.

To further examine the role of ADK in MT dynamics, ADK was over-expressed in cardiomyocytes using adenovirus. Over-expression of ADK had no significant effect on total α-tubulin levels in the soluble or CSK fraction as compared to β-gal infected cells (figure 7A, B, C), but did enhance CADO induced reductions in cytoskeletal tubulin (figure 7A, C) and detyrosinated tubulin within the soluble fraction (figure 7A, D). At the same time, ADK had little observable effect on desmin or β-actin polymerization (figure 7A). Interestingly, immunofluorescent analysis demonstrated that ADK over-expression, even in absence of exogenous adenosine, promoted microtubule disorganization that was characterized by reduced microtubule alignment and failure of detyrosinated MTs to extend into the cytosol (figure 7F), suggesting ADK regulates both cardiomyocyte MT stability and MT organization. Because microtubule organization plays an important role in cell enlargement, we examined how ADK over-expression impacts cardiomyocyte hypertrophy. Interestingly, ADK over-expression limited phenylephrine induced cardiomyocyte enlargement in absence of exogenous adenosine, and potentiated CADO attenuation of cell enlargement, while ADK inhibition with ABT-702 mostly reversed the effects of CADO (figure 7G). These data indicate that ADK metabolism of adenosine attenuates microtubule stabilization and hypertrophy in cardiomyocytes.

Discussion

This study identifies a novel role for ADK-dependent adenosine metabolism in cardiomyocyte homeostasis and functional adaptation to LV pressure overload. Cardiomyocyte-specific ADK knockout caused cardiomyocyte hypertrophy under basal conditions and significantly exacerbated TAC induced hypertrophy and LV dysfunction. In addition to increasing mTORC1 and ERK signaling, ADK disruption promoted microtubule detyrosination, a post-translational microtubule modification observed in human heart failure of multiple etiologies that is believed to impair cardiomyocyte contractility [13, 15]. Thus ADK activity, ostensibly through its phosphorylation of adenosine, plays a homeostatic role in the heart, dampening both cardiac growth signaling (mTORC1 and ERK) and excessive microtubule stabilization/detyrosination. Together, these findings identify ADK as a novel regulator of cardiomyocyte microtubule dynamics that protects against pathological hypertrophy.

While the specific molecular mechanisms underlying ADK attenuation of cardiac hypertrophy are unclear, ADK down-regulation of mTORC1 signaling is likely a contributing factor. mTORC1 is a protein complex which activates p70S6 kinase and inhibits 4E-BP, facilitating ribosomal biogenesis, protein translation, and other anabolic actions [31, 44]. mTORC1 activity is necessary for compensatory hypertrophy[32] and inhibition of mTORC1 signaling with rapamycin has been shown to attenuate pressure overload induced cardiac hypertrophy [29]. The finding that ADK disruption increased mTORC1 activity is consistent with our previous findings in neonatal cardiomyocytes showing that CADO-mediated inhibition of mTORC1 signaling was restored by ADK inhibition with iodotubercidin[20]. However, unlike our findings in cultured cells, much of the increase in mTORC1 signaling in cADK$^{-/-}$ hearts appeared due to increased expression level of mTORC1 signaling components. In addition to regulating anabolic signaling in the heart, ADK activity limits mTORC1 signaling in the pancreas, where in vivo administration of

ADK inhibitors promote islet beta cell replication[45]. p44/42 ERK MAP kinase was also upregulated in cADK$^{-/-}$ hearts at the protein level, resulting in constitutively higher phosphorylated ERK content. Both ERK and mTORC1 signaling promote cardiac hypertrophy[29, 30] but also protect against cell death and preserve cardiac function in the setting of pressure overload[32, 46, 47]. Thus, activation of these pathways may contribute to increased hypertrophy and enhanced activation of the fetal gene program in cADK$^{-/-}$ hearts, but their known cardio-protective actions suggest they are not likely the primary cause of cADK$^{-/-}$ LV dysfunction .

A more likely factor in the LV dysfunction observed in cADK$^{-/-}$ mice after pressure overload is increased stabilization and accumulation of cardiac microtubules. Cardiomyocyte microtubule densification is induced by ventricular pressure overload in many animal species [4835][11, 12] and is also observed in samples from patients in end stage heart failure[49, 50]. Recently, the impact of cardiac microtubule stabilization on LV function has gained more recognition, as elegant live cell microtubule imaging and single cell measurements of contractility have specifically identified detyrosinated microtubules as a source of mechanical impairment in cardiomyocytes isolated from mouse or human failing hearts[13, 15]. cADK$^{-/-}$ hearts exposed to TAC exhibit reduced ejection fraction and impaired relaxation, which are consistent with an increase in cardiomyocyte viscosity. The finding that TAC-induced fibrosis was not worsened by ADK disruption suggests cell death or inflammation were not exacerbated by ADK disruption and points towards an intra-cardiomyocyte mechanism of impaired contractility. In addition to increasing myofilament load, stabilized microtubules can dysregulate stretch induced calcium dynamics through a process known as X-ROS signaling[17, 18]. Pressure overload induced microtubule stabilization can also interfere with trafficking of junctophillin to the SR, leading to disrupted SR architecture and altered calcium dynamics[36]. Thus, aberrant MT stabilization/redistribution in cADK$^{-/-}$ hearts could impair contractility through dysregulated calcium handling and/or increased viscous load. In support of a maladaptive role for pressure overload-induced subcellular redistribution of MTs, our lab observed that tubulin accumulation in the membrane and cytoskeletal fractions of ventricular MT preparations correlated strikingly with impaired LV function during pressure overload[37]. The finding that ventricular ADK expression increased in response to moderate TAC suggests an adaptive role for ADK in preservation of normal MT dynamics during cardiac stress, as WT mice showed almost no increase in microtubule stabilization or redistribution and no impairment of LV function in response to TAC. Loss of ADK activity on the other hand, increased MT stabilization, detyrosination, and subcellular redistribution, even in absence of stress.

Interestingly, despite having increased detyrosinated microtubules under basal conditions, LV dysfunction was not observed in cADK$^{-/-}$ hearts until pressure overload was applied. This might argue against a prominent role for MT detyrosination in contractile impairment. However, it is possible that the spontaneous hypertrophy observed in cADK$^{-/-}$ hearts developed, in part, as a compensatory response to overcome MT induced contractile impairment. Notably, cardiac hypertrophy was also observed in a transgenic mouse model expressing a microtubule stabilizing tubulin mutation in the heart[12]. In addition, cADK$^{-/-}$ hearts exhibited increased levels of desmin and β-actin under basal conditions, while desmin expression was further increased in cADK$^{-/-}$ hearts after TAC. A previous study showed

that exogenously expressed β-actin can increase adult cardiomyocyte contractility[51]. Interactions between sarcomeric desmin and detyrosinated MTs, however, are believed to increase viscous load on myofilaments[13]. Increased desmin levels accompanied by increased detyrosinated tubulin in cADK$^{-/-}$ hearts after TAC may also contribute to the observed LV dysfunction in these mice.

In cultured neonatal cardiomyocytes, treatment with adenosine or 2-CADO reduced detyrosinated microtubules through an ADK dependent mechanism. Together, with the observation of increased MT stability and redistribution in cADK$^{-/-}$ hearts, these findings suggest ADK metabolism of endogenous, intracellular adenosine, and presumably, production of AMP, limits MT stabilization to maintain MT dynamics. Though we previously demonstrated that AMPK can attenuate microtubule stabilization[52], AMPK phosphorylation was only modestly affected in cADK$^{-/-}$ hearts. Expression of tubulin tyrosine ligase and vasohibin1, enzymes that mediate tubulin re-tyrosination or MT detyrosination, respectively, also were not altered in cADK$^{-/-}$ hearts in a manner that would promote MT detyrosination. Our findings that ADK disruption increases cardiac MT stability and alters subcellular tubulin distribution in vivo, and that over-expression of ADK causes MT disorganization in NRVMs (in addition to reducing detyrosinated tubulin), suggests ADK activity may modulate the function of a protein(s) that modulates both MT stability and tracking. Because ADK is localized in the nucleus in cardiomyocytes, and extracellular adenosine is converted to ATP in the nucleus[53], we hypothesize that ADK may modulate MT stability by regulating the activity of a perinuclear MT-depolymerizing kinesin or other MT-associated protein that is sensitive to changes in perinuclear adenine nucleotides. The molecular mechanism(s) underlying the striking effects of ADK-mediated adenosine metabolism on microtubules and cardiomyocyte hypertrophy will be the subject of future studies.

Conclusion

ADK activity attenuates cardiac hypertrophy and is important for physiological adaptation to pressure overload. ADK activity also mediates adenosine suppression of microtubule stability/detyrosination, suggesting a novel link between adenosine recycling and microtubule dynamics. Strategies to increase myocardial adenosine metabolism by ADK could therefore provide a new approach to attenuate cardiomyocyte microtubule detyrosination, limit hypertrophy, and improve cardiomyocyte contractility in the failing heart.

Supplementary Material

Refer to Web version on PubMed Central for supplementary material.

Acknowledgments

Financial support: HL20598, HL21872 and HL71790 from the National Heart, Lung, and Blood Institute. Drs Zhang, Fassett are recipients of Scientist Development Awards from the American Heart Association. Drs. Fassett and Mayer are recipients of an Austrian Science Foundation grant, FWF Project P 31083-B34

References

1. Solenkova NV, Solodushko V, Cohen MV and Downey JM. Endogenous adenosine protects preconditioned heart during early minutes of reperfusion by activating Akt. Am J Physiol Heart Circ Physiol 2006;290:H441–9. [PubMed: 16155103]
2. Headrick JP and Lasley RD. Adenosine receptors and reperfusion injury of the heart. Handb Exp Pharmacol 2009:189–214. [PubMed: 19639283]
3. Mustafa SJ, Morrison RR, Teng B and Pelleg A. Adenosine receptors and the heart: role in regulation of coronary blood flow and cardiac electrophysiology. Handb Exp Pharmacol 2009:161–88. [PubMed: 19639282]
4. Hasko G and Pacher P. A2A receptors in inflammation and injury: lessons learned from transgenic animals. J Leukoc Biol 2008;83:447–55. [PubMed: 18160539]
5. Linden J and Cekic C. Regulation of lymphocyte function by adenosine. Arterioscler Thromb Vasc Biol 2012;32:2097–103. [PubMed: 22772752]
6. Dubey RK, Gillespie DG and Jackson EK. Adenosine inhibits collagen and protein synthesis in cardiac fibroblasts: role of A2B receptors. Hypertension 1998;31:943–8. [PubMed: 9535419]
7. Liao Y, Takashima S, Asano Y, Asakura M, Ogai A, Shintani Y, Minamino T, Asanuma H, Sanada S, Kim J, Ogita H, Tomoike H, Hori M and Kitakaze M. Activation of adenosine A1 receptor attenuates cardiac hypertrophy and prevents heart failure in murine left ventricular pressure-overload model. Circ Res 2003;93:759–66. [PubMed: 12970111]
8. Sassi Y, Ahles A, Truong DJ, Baqi Y, Lee SY, Husse B, Hulot JS, Foinquinos A, Thum T, Muller CE, Dendorfer A, Laggerbauer B and Engelhardt S. Cardiac myocyte-secreted cAMP exerts paracrine action via adenosine receptor activation. J Clin Invest 2014;124:5385–97. [PubMed: 25401477]
9. Xu X, Fassett J, Hu X, Zhu G, Lu Z, Li Y, Schnermann J, Bache RJ and Chen Y. Ecto-5'-nucleotidase deficiency exacerbates pressure-overload-induced left ventricular hypertrophy and dysfunction. Hypertension 2008;51:1557–64. [PubMed: 18391093]
10. Lu Z, Fassett J, Xu X, Hu X, Zhu G, French J, Zhang P, Schnermann J, Bache RJ and Chen Y. Adenosine A3 receptor deficiency exerts unanticipated protective effects on the pressure-overloaded left ventricle. Circulation 2008;118:1713–21. [PubMed: 18838560]
11. Fassett JT, Xu X, Hu X, Zhu G, French J, Chen Y and Bache RJ. Adenosine regulation of microtubule dynamics in cardiac hypertrophy. Am J Physiol Heart Circ Physiol 2009;297:H523–32. [PubMed: 19525375]
12. Cheng G, Zile MR, Takahashi M, Baicu CF, Bonnema DD, Cabral F, Menick DR and Cooper Gt. A direct test of the hypothesis that increased microtubule network density contributes to contractile dysfunction of the hypertrophied heart. Am J Physiol Heart Circ Physiol 2008;294:H2231–41. [PubMed: 18344371]
13. Robison P, Caporizzo MA, Ahmadzadeh H, Bogush AI, Chen CY, Margulies KB, Shenoy VB and Prosser BL. Detyrosinated microtubules buckle and bear load in contracting cardiomyocytes. Science 2016;352:aaf0659.
14. Tsutsui H, Ishihara K and Cooper Gt. Cytoskeletal role in the contractile dysfunction of hypertrophied myocardium. Science 1993;260:682–7. [PubMed: 8097594]
15. Chen CY, Caporizzo MA, Bedi K, Vite A, Bogush AI, Robison P, Heffler JG, Salomon AK, Kelly NA, Babu A, Morley MP, Margulies KB and Prosser BL. Suppression of detyrosinated microtubules improves cardiomyocyte function in human heart failure. Nat Med 2018.
16. Hong TT, Smyth JW, Gao D, Chu KY, Vogan JM, Fong TS, Jensen BC, Colecraft HM and Shaw RM. BIN1 localizes the L-type calcium channel to cardiac T-tubules. PLoS Biol 8:e1000312.
17. Prosser BL, Khairallah RJ, Ziman AP, Ward CW and Lederer WJ. X-ROS signaling in the heart and skeletal muscle: stretch-dependent local ROS regulates [Ca(2)(+)]i. J Mol Cell Cardiol 2013;58:172–81. [PubMed: 23220288]
18. Kerr JP, Robison P, Shi G, Bogush AI, Kempema AM, Hexum JK, Becerra N, Harki DA, Martin SS, Raiteri R, Prosser BL and Ward CW. Detyrosinated microtubules modulate mechanotransduction in heart and skeletal muscle. Nature communications 2015;6:8526.

19. Peart J, Willems L and Headrick JP. Receptor and non-receptor-dependent mechanisms of cardioprotection with adenosine. Am J Physiol Heart Circ Physiol 2003;284:H519–27. [PubMed: 12388277]

20. Fassett JT, Hu X, Xu X, Lu Z, Zhang P, Chen Y and Bache RJ. Adenosine kinase regulation of cardiomyocyte hypertrophy. Am J Physiol Heart Circ Physiol 2011;300:H1722–32. [PubMed: 21335462]

21. Kroll K, Decking UK, Dreikorn K and Schrader J. Rapid turnover of the AMP-adenosine metabolic cycle in the guinea pig heart. Circ Res 1993;73:846–56. [PubMed: 8403255]

22. Boyle DL, Kowaluk EA, Jarvis MF, Lee CH, Bhagwat SS, Williams M and Firestein GS. Anti-inflammatory effects of ABT-702, a novel non-nucleoside adenosine kinase inhibitor, in rat adjuvant arthritis. J Pharmacol Exp Ther 2001;296:495–500. [PubMed: 11160636]

23. Elsherbiny NM, Ahmad S, Naime M, Elsherbini AM, Fulzele S, Al-Gayyar MM, Eissa LA, El-Shishtawy MM and Liou GI. ABT-702, an adenosine kinase inhibitor, attenuates inflammation in diabetic retinopathy. Life Sci 2013;93:78–88. [PubMed: 23770229]

24. Boison D Adenosine kinase: exploitation for therapeutic gain. Pharmacological reviews 2013;65:906–43. [PubMed: 23592612]

25. Deussen A, Stappert M, Schafer S and Kelm M. Quantification of extracellular and intracellular adenosine production: understanding the transmembranous concentration gradient. Circulation 1999;99:2041–7. [PubMed: 10209010]

26. Sohal DS, Nghiem M, Crackower MA, Witt SA, Kimball TR, Tymitz KM, Penninger JM and Molkentin JD. Temporally regulated and tissue-specific gene manipulations in the adult and embryonic heart using a tamoxifen-inducible Cre protein. Circ Res 2001;89:20–5. [PubMed: 11440973]

27. Hu P, Zhang D, Swenson L, Chakrabarti G, Abel ED and Litwin SE. Minimally invasive aortic banding in mice: effects of altered cardiomyocyte insulin signaling during pressure overload. Am J Physiol Heart Circ Physiol 2003;285:H1261–9. [PubMed: 12738623]

28. Khairallah RJ, Shi G, Sbrana F, Prosser BL, Borroto C, Mazaitis MJ, Hoffman EP, Mahurkar A, Sachs F, Sun Y, Chen YW, Raiteri R, Lederer WJ, Dorsey SG and Ward CW. Microtubules underlie dysfunction in duchenne muscular dystrophy. Sci Signal 2012;5:ra56.

29. Shioi T, McMullen JR, Tarnavski O, Converso K, Sherwood MC, Manning WJ and Izumo S. Rapamycin attenuates load-induced cardiac hypertrophy in mice. Circulation 2003;107:1664–70. [PubMed: 12668503]

30. Bueno OF, De Windt LJ, Tymitz KM, Witt SA, Kimball TR, Klevitsky R, Hewett TE, Jones SP, Lefer DJ, Peng CF, Kitsis RN and Molkentin JD. The MEK1-ERK1/2 signaling pathway promotes compensated cardiac hypertrophy in transgenic mice. EMBO J 2000;19:6341–50. [PubMed: 11101507]

31. Sciarretta S, Volpe M and Sadoshima J. Mammalian target of rapamycin signaling in cardiac physiology and disease. Circ Res 2014;114:549–64. [PubMed: 24481845]

32. Zhang D, Contu R, Latronico MV, Zhang J, Rizzi R, Catalucci D, Miyamoto S, Huang K, Ceci M, Gu Y, Dalton ND, Peterson KL, Guan KL, Brown JH, Chen J, Sonenberg N and Condorelli G. MTORC1 regulates cardiac function and myocyte survival through 4E-BP1 inhibition in mice. J Clin Invest 2010;120:2805–16. [PubMed: 20644257]

33. Zhang P, Hu X, Xu X, Fassett J, Zhu G, Viollet B, Xu W, Wiczer B, Bernlohr DA, Bache RJ and Chen Y. AMP activated protein kinase-alpha2 deficiency exacerbates pressure-overload-induced left ventricular hypertrophy and dysfunction in mice. Hypertension 2008;52:918–24. [PubMed: 18838626]

34. Boison D, Scheurer L, Zumsteg V, Rulicke T, Litynski P, Fowler B, Brandner S and Mohler H. Neonatal hepatic steatosis by disruption of the adenosine kinase gene. Proc Natl Acad Sci U S A 2002;99:6985–90. [PubMed: 11997462]

35. Tagawa H, Koide M, Sato H, Zile MR, Carabello BA and Cooper Gt. Cytoskeletal role in the transition from compensated to decompensated hypertrophy during adult canine left ventricular pressure overloading. Circ Res 1998;82:751–61. [PubMed: 9562434]

36. Zhang C, Chen B, Guo A, Zhu Y, Miller JD, Gao S, Yuan C, Kutschke W, Zimmerman K, Weiss RM, Wehrens XH, Hong J, Johnson FL, Santana LF, Anderson ME and Song LS. Microtubule-

Mediated Defects in Junctophilin-2 Trafficking Contribute to Myocyte T-Tubule Remodeling and Ca2+ Handling Dysfunction in Heart Failure. Circulation 2014.

37. Fassett JT, Xu X, Kwak D, Wang H, Liu X, Hu X, Bache RJ and Chen Y. Microtubule Actin Cross-linking Factor 1 regulates cardiomyocyte microtubule distribution and adaptation to hemodynamic overload. PLoS One 2013;8:e73887. [PubMed: 24086300]
38. Gundersen GG and Bulinski JC. Microtubule arrays in differentiated cells contain elevated levels of a post-translationally modified form of tubulin. Eur J Cell Biol 1986;42:288–94. [PubMed: 3545837]
39. Dunn S, Morrison EE, Liverpool TB, Molina-Paris C, Cross RA, Alonso MC and Peckham M. Differential trafficking of Kif5c on tyrosinated and detyrosinated microtubules in live cells. J Cell Sci 2008;121:1085–95. [PubMed: 18334549]
40. Lin SX, Gundersen GG and Maxfield FR. Export from pericentriolar endocytic recycling compartment to cell surface depends on stable, detyrosinated (glu) microtubules and kinesin. Mol Biol Cell 2002;13:96–109. [PubMed: 11809825]
41. Nieuwenhuis J and Brummelkamp TR. The Tubulin Detyrosination Cycle: Function and Enzymes. Trends Cell Biol 2019;29:80–92. [PubMed: 30213517]
42. Aillaud C, Bosc C, Peris L, Bosson A, Heemeryck P, Van Dijk J, Le Friec J, Boulan B, Vossier F, Sanman LE, Syed S, Amara N, Coute Y, Lafanechere L, Denarier E, Delphin C, Pelletier L, Humbert S, Bogyo M, Andrieux A, Rogowski K and Moutin MJ. Vasohibins/SVBP are tubulin carboxypeptidases (TCPs) that regulate neuron differentiation. Science 2017;358:1448–1453. [PubMed: 29146868]
43. Nieuwenhuis J, Adamopoulos A, Bleijerveld OB, Mazouzi A, Stickel E, Celie P, Altelaar M, Knipscheer P, Perrakis A, Blomen VA and Brummelkamp TR. Vasohibins encode tubulin detyrosinating activity. Science 2017;358:1453–1456. [PubMed: 29146869]
44. Ben-Sahra I and Manning BD. mTORC1 signaling and the metabolic control of cell growth. Curr Opin Cell Biol 2017;45:72–82. [PubMed: 28411448]
45. Annes JP, Ryu JH, Lam K, Carolan PJ, Utz K, Hollister-Lock J, Arvanites AC, Rubin LL, Weir G and Melton DA. Adenosine kinase inhibition selectively promotes rodent and porcine islet beta-cell replication. Proc Natl Acad Sci U S A 2012;109:3915–20. [PubMed: 22345561]
46. Purcell NH, Wilkins BJ, York A, Saba-El-Leil MK, Meloche S, Robbins J and Molkentin JD. Genetic inhibition of cardiac ERK1/2 promotes stress-induced apoptosis and heart failure but has no effect on hypertrophy in vivo. Proc Natl Acad Sci U S A 2007;104:14074–9. [PubMed: 17709754]
47. Song X, Kusakari Y, Xiao CY, Kinsella SD, Rosenberg MA, Scherrer-Crosbie M, Hara K, Rosenzweig A and Matsui T. mTOR attenuates the inflammatory response in cardiomyocytes and prevents cardiac dysfunction in pathological hypertrophy. American journal of physiology Cell physiology 2010;299:C1256–66. [PubMed: 20861467]
48. Tsutsui H, Tagawa H, Kent RL, McCollam PL, Ishihara K, Nagatsu M and Cooper Gt. Role of microtubules in contractile dysfunction of hypertrophied cardiocytes. Circulation 1994;90:533–55. [PubMed: 8026043]
49. Heling A, Zimmermann R, Kostin S, Maeno Y, Hein S, Devaux B, Bauer E, Klovekorn WP, Schlepper M, Schaper W and Schaper J. Increased expression of cytoskeletal, linkage, and extracellular proteins in failing human myocardium. Circ Res 2000;86:846–53. [PubMed: 10785506]
50. Aquila-Pastir LA, DiPaola NR, Matteo RG, Smedira NG, McCarthy PM and Moravec CS. Quantitation and distribution of beta-tubulin in human cardiac myocytes. J Mol Cell Cardiol 2002;34:1513–23. [PubMed: 12431450]
51. Balasubramanian S, Mani SK, Kasiganesan H, Baicu CC and Kuppuswamy D. Hypertrophic stimulation increases beta-actin dynamics in adult feline cardiomyocytes. PloS one 2010;5:e11470. [PubMed: 20635003]
52. Fassett JT, Hu X, Xu X, Lu Z, Zhang P, Chen Y and Bache RJ. AMPK attenuates microtubule proliferation in cardiac hypertrophy. Am J Physiol Heart Circ Physiol 2013;304:H749–58. [PubMed: 23316058]

53. Rapaport E Compartmentalized ATP pools produced from adenosine are nuclear pools. J Cell Physiol 1980;105:267–74. [PubMed: 6450772]

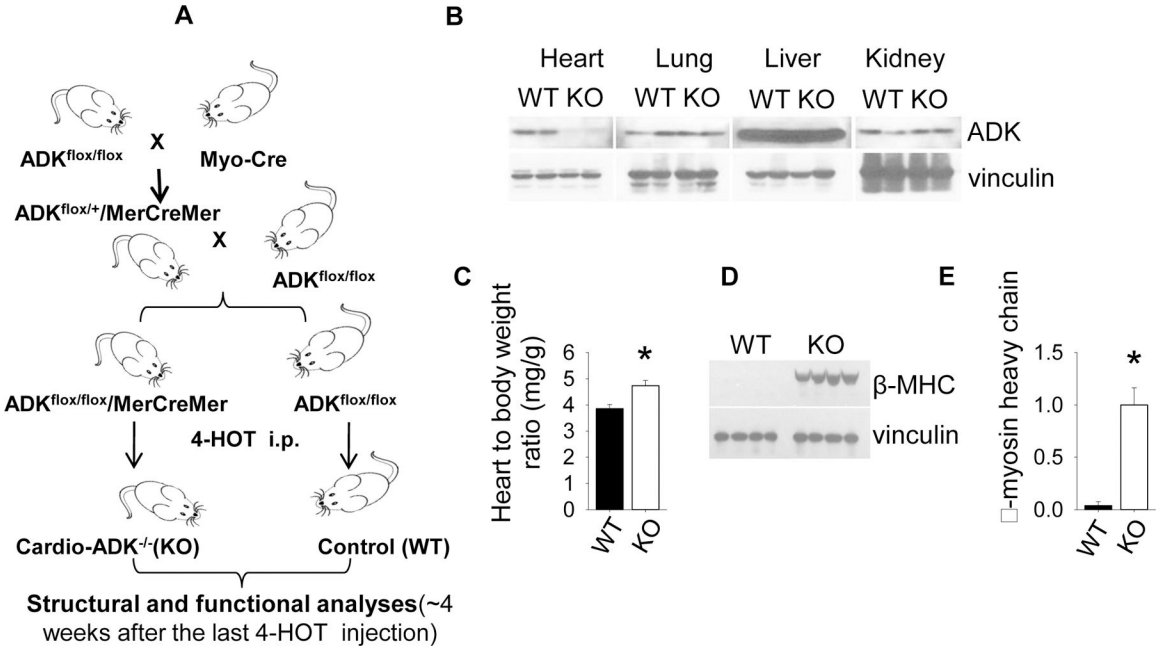

Figure 1.

Cardiomyocyte specific ADK disruption causes spontaneous LV hypertrophy. **(A)** Tamoxifen induced cardiomyocyte specific excision of floxed exon 7 in the ADK gene. **(B)** 4 weeks after the last tamoxifen injection, ADK protein expression was eliminated specifically in heart muscle in $cADK^{-/-}$ mice. **(C)** Heart weight to body weight ratio of $cADK^{-/-}$ and WT mice (n=9 WT and 10 $cADK^{-/-}$). **(D**, **E)** β-MHC expression in WT and $cADK^{-/-}$ was analyzed by western blot (n=4 WT and 4 $ADK^{-/-}$).

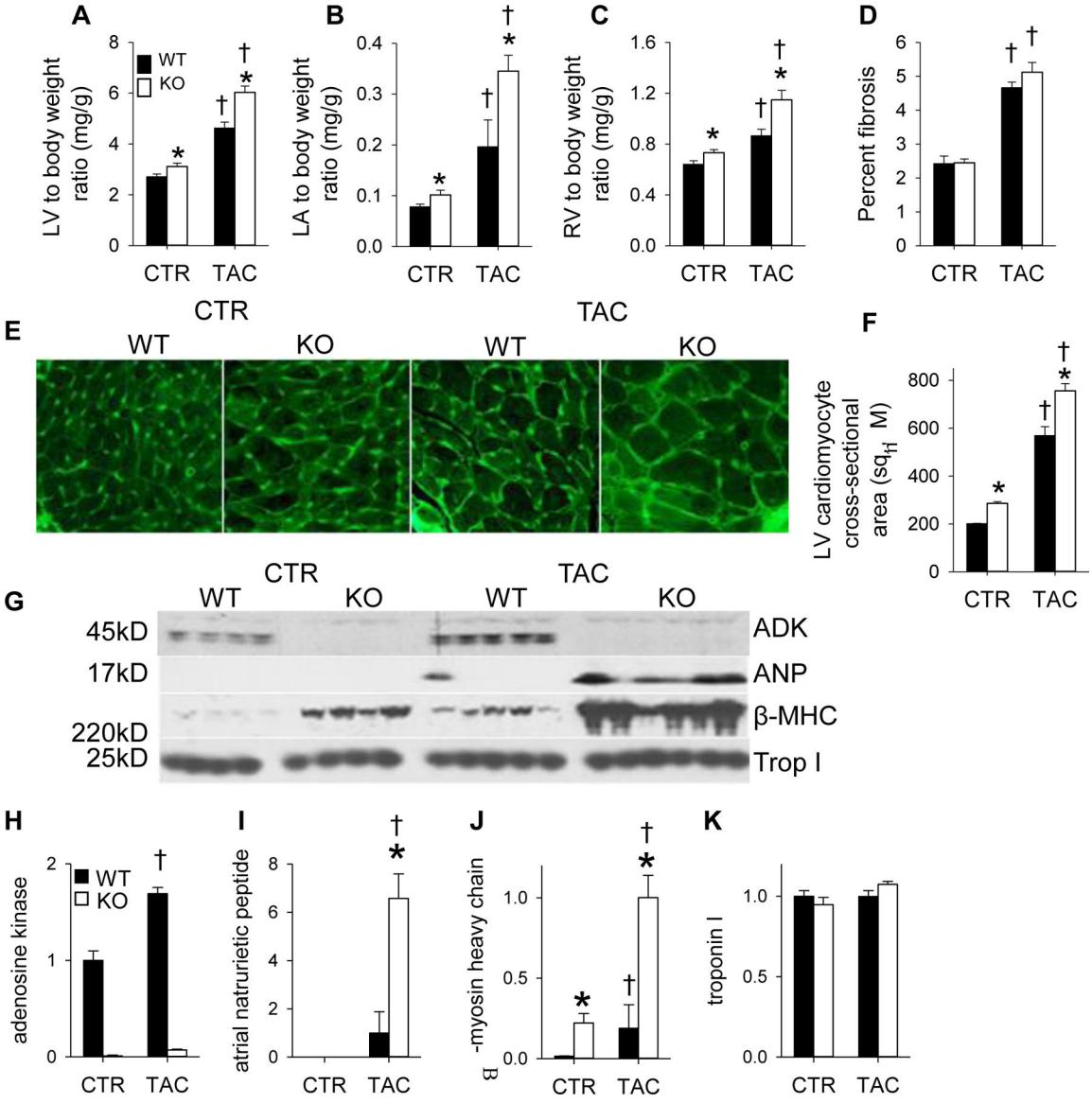

Figure 2. Cardiomyocyte ADK expression increases in response to LV pressure overload and attenuates pressure overload induced LV hypertrophy and fetal gene program.

(A) LV, **(B)** LA, and **(C)** RV weight to body weight ratios in WT and cADK$^{-/-}$ mice after 6 weeks of control or pressure overload (TAC) conditions. (n=26, 24, 17, and 17 for WT, ADK$^{-/-}$, WT-TAC, and ADK$^{-/-}$-TAC, respectively) **(D)** Quantitation of fibrosis in LV sections from WT and cADK$^{-/-}$ hearts (n=5, 5, 5, and 5 for WT. ADK$^{-/-}$, WT-TAC, and ADK$^{-/-}$-TAC, respectively) **(E, F)** WGA stain and LV cardiomyocyte cross-sectional area from WT and cADK$^{-/-}$ hearts under control or TAC conditions (n=5, 5, 5, and 5 for WT. ADK$^{-/-}$, WT-TAC, and ADK$^{-/-}$-TAC, respectively) **(G)** Western blot and quantitation of **(H)**, ADK **(I)**, beta myosin heavy chain (-MHC) **(J)**, atrial natruretic peptide (ANP) and **(K)** troponin I (n=5, 5, 6, 7 for WT, ADK$^{-/-}$, WT-TAC, and ADK$^{-/-}$-TAC respectively).

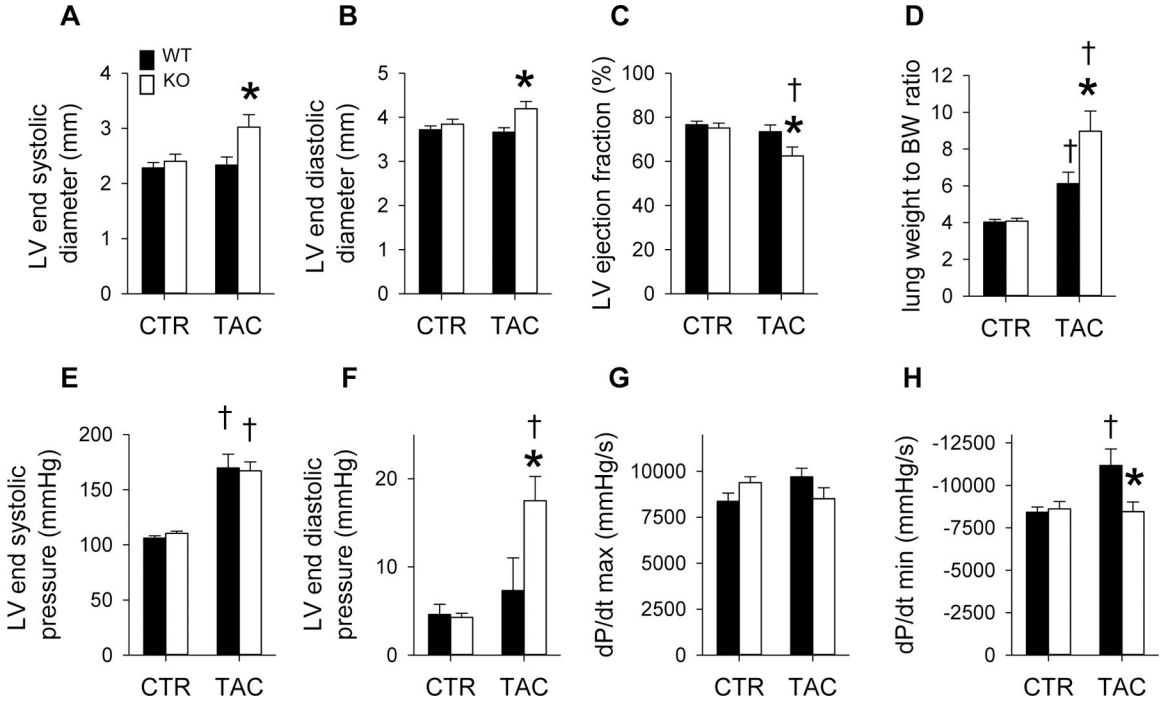

Figure 3. Effects of cardiomyocyte ADK disruption on LV function during pressure overload

(A) Echocardiography measurements of end systolic diameter (ESD), **(B)** end diastolic diameter (EDD) and **(C)** ejection fraction (EF) 6 weeks after sham or TAC surgery. (n=10, 11, 12, and 14 for WT. ADK$^{-/-}$, WT-TAC, and ADK$^{-/-}$-TAC, respectively) **(D)** Lung weight to body weight ratio in WT and cADK$^{-/-}$ mice 6 weeks after TAC (n= 26, 24, 17, and 17 for, WT, ADK$^{-/-}$, WT-TAC, and ADK$^{-/-}$-TAC, respectively). **(E)** Left ventricular end systolic and **(F)** diastolic pressures and rates of LV pressure development during **(G)** systole and **(H)** diastole in WT and cADK$^{-/-}$ mice after TAC. (n=8, 9, 6, and 10 for WT. ADK$^{-/-}$, WT-TAC, and ADK$^{-/-}$-TAC, respectively)

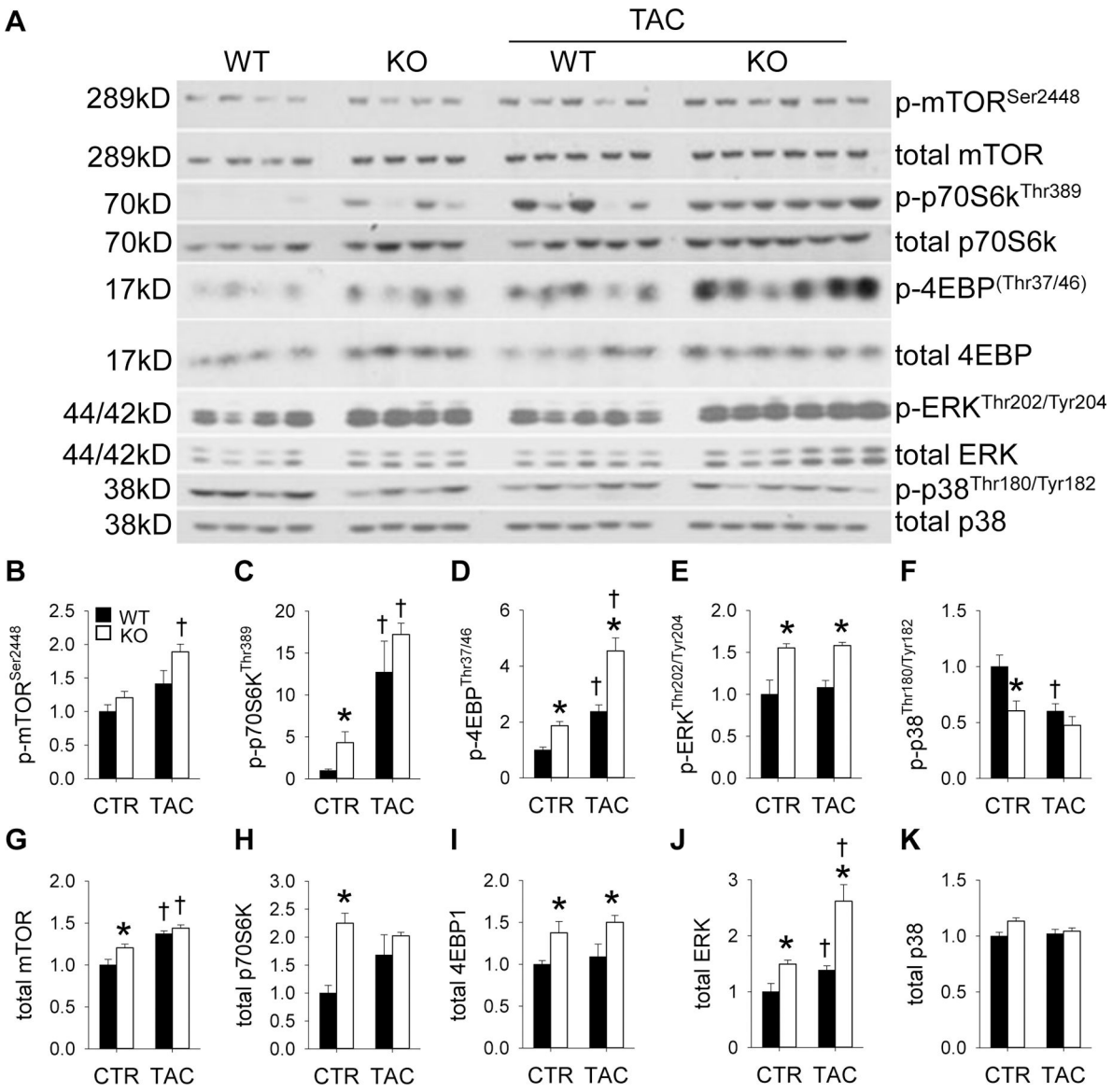

Figure 4. Cardiac mTORC1 and p44/42 ERK MAP kinase pathways are upregulated by ADK disruption

(A-B) 6 weeks after TAC or sham surgeries, WT and cADK$^{-/-}$ ventricular lysates were analyzed by western blot for phosphorylated and total levels of mTOR^{Ser2448}**(A, B, G)**, p70S6k^{Thr389} **(A, C, H)**, 4E-BP$^{Thr37/46}$**(A, D, I)** MAP kinases ERK$^{Thr202/Tyr204}$ **(A, E, J)** and p38$^{Thr180/Tyr182}$ **(A, F, K)** in WT and cADK$^{-/-}$ ventricular lysates under control and TAC conditions. (n=5, 5, 6, and 7 for WT. cADK$^{-/-}$, WT-TAC, and cADK$^{-/-}$-TAC respectively).

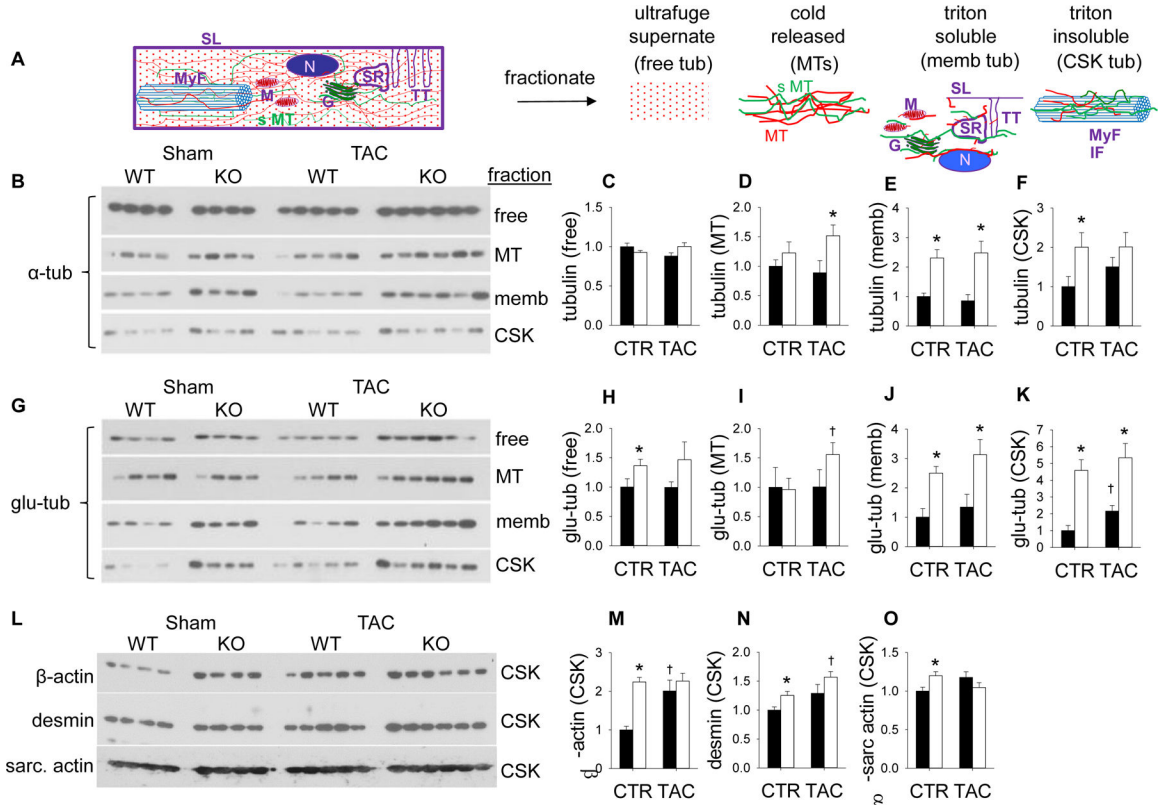

Figure 5. ADK disruption increases microtubule stabilization/detyrosination

(A) Ventricular lysates were separated into different Free, Microtubule (MT), Membrane (Memb), and Cytoskeletal (CSK) fractions as depicted. (N is nucleus, G is golgi, SR is sarcoplasmic reticulum, TT is t-tubules, M is mitochondria, SL is sarcolemma, CSK is cytoskeleton, MT is microtubule, and sMT is stabilized microtubule). Cardiac lysates were analyzed by western blot for alpha tubulin **(B–F)** and detyrosinated tubulin (Glu-tubulin) **(G–K)**. β-actin **(L,M)**, desmin **(L, N)** and sarcomeric actin **(L,O)**, were also measured in the triton insoluble cytoskeletal fraction. (n=4, 4, 5, and 6 for WT. cADK$^{-/-}$, WT-TAC, and cADK$^{-/-}$ TAC respectively).

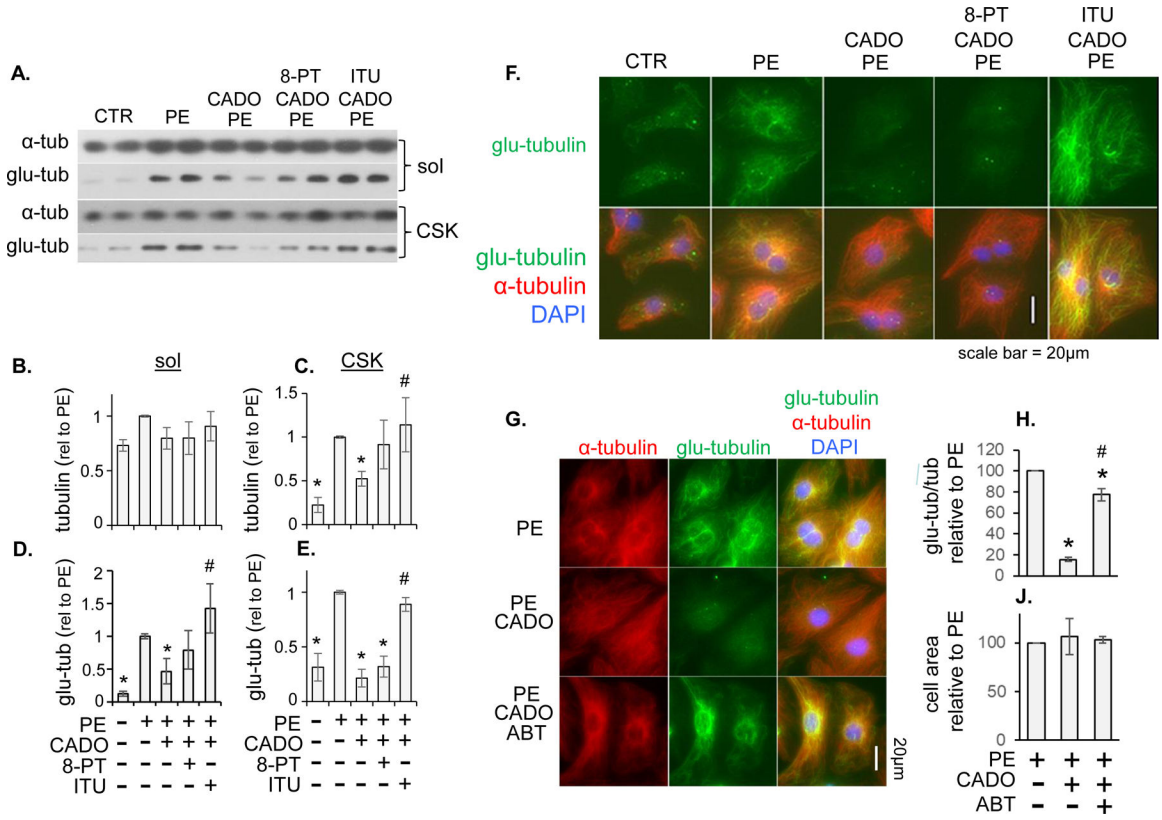

Figure 6. Pharmacological inhibition of ADK reverses CADO attenuation of microtubule stabilization/detyrosination.

(A) Neonatal cardiomyocytes (NRVMs) were treated with phenylephrine (50 μM) for 48 hours in presence of CADO (5 μM), CADO + non-selective adenosine receptor antagonist 8-PT (10 μM), or CADO + ADK inhibitor iodotubercidin (ITU; 0.3 μM). α-tubulin (**B** and **C**) and detyrosinated α-tubulin (glu-tubulin) (**D** and **E**) were measured by western blot in triton soluble (sol) (**B** and **D**) and insoluble (CSK) (**C** and **E**) fractions (n ≥ 4 per condition. * indicates $p < .05$ compared to PE. # indicates $p < .05$ compared to PE-CADO). **(F)** Immunofluorescence staining of NRVMs for α-tubulin and glu-tubulin after treatment described above. **(G)** NRVMs were treated with PE for 48 hours to induce hypertrophy, followed by an additional 24 hours with PE, PE + CADO, or PE + CADO + ABT-702(0.3 μM). α-tubulin and glu-tubulin were visualized by immunofluorescence and the area of detyrosinated tubulin was divided by the area of total tub **(H)** in 25–30 cells per condition. Percent change in cell area was also measured **(J)**. Results are the average of 3 experiments, relative to continued PE treatment alone

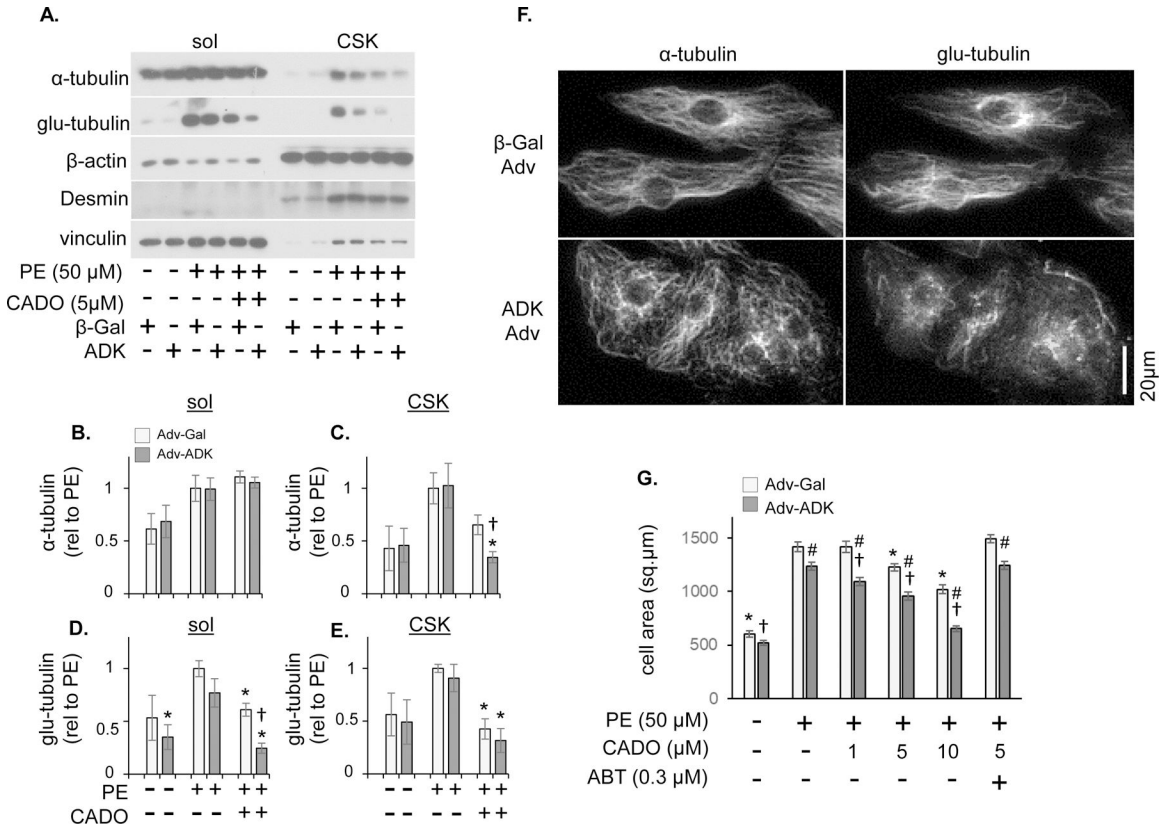

Figure 7. ADK adenovirus augments CADO suppression of microtubule stabilization/ detyrosination.

(A) Neonatal cardiomyocytes (NRVMs) were infected with β-gal or ADK expressing adenovirus (adv) for 24 hours prior to treatment with PE for 48 hours in the presence or absence of CADO (5 μM). Soluble **(A, B, D)** and cytoskeletal fractions **(B, C, E)** were examined by western blot for α-tubulin and glu-tubulin. CADO + non-selective adenosine receptor antagonist 8-PT (10 μM), or CADO + ADK inhibitor iodotubercidin (ITU; 0.3 μM). α-tubulin (**B** and **C**) and detyrosinated α-tubulin (glu-tubulin) (**D** and **E**) were measured by western blot in triton soluble (sol) (**B** and **D**) and insoluble (CSK) (**C** and **E**) fractions ($n \geq 4$ per condition. * indicates $p<.05$ compared to PE. † indicates $p<.05$ compared to PE-CADO). **(F)** NRVMs infected with β-gal or ADK adv were examined by immunofluorescence for α-tubulin and glu-tubulin. **(G)** Cell area was measured in NRVMs infected with β-gal or ADK adv 48 hours after treatment with PE, PE + 1, 5, or 10 M CADO, or PE + 5 μM CADO + 0.3 μM ABT-702. (Bars represent the average cell area of at least 100 cells measured per condition; (* indicates $p<.05$ compared to PE. indicates $p<.05$ compared to PE-CADO. # indicates $p<.05$ comparing ADK adv to β-gal adv under same treatment)